

# Sensitivity Analysis of Frequency Regulation Parameters in Power Systems with Wind Generation



Julian Patiño, José David López and Jairo Espinosa

**Abstract** In power systems, frequency constitutes a parameter indicating the equilibrium between power demanded by load and energy produced by generation systems. This chapter studies the effects of varying different system parameters on the overall performance of the traditional frequency regulation system when including contributions of renewable energy sources. A model for the inclusion of variable speed wind turbines in the frequency control loops is analyzed, and parametric sensitivity functions are established using linearized models and transfer function representations for the system components. Through both theoretical analysis and performance simulations, the impact of an inaccurate representation of system inertia in frequency performance is established. Stability analysis for inertia sensitivity of frequency regulation involving wind generation is also provided. Results indicate more robustness to parameter variations for systems including wind turbine participation. However, the frequency deviation rate increases when the uncertainty in system parameters grows. This behavior might lead to instability scenarios under frequency disturbances for the power system.

## 1 Introduction

In power systems, frequency constitutes a parameter indicating the equilibrium between power demanded by load and energy produced by generation systems [1]. When this relationship is unbalanced, control structures are in place to return the

---

J. Patiño (✉) · J. Espinosa  
Universidad Nacional de Colombia, Manizales, Colombia  
e-mail: [japatin0@unal.edu.co](mailto:japatin0@unal.edu.co)

J. Espinosa  
e-mail: [jespinov@unal.edu.co](mailto:jespinov@unal.edu.co)

J. Patiño  
I. U. Pascual Bravo, Calle 73 No. 73A-226, Medellín, Colombia

J. D. López  
Universidad de Antioquia UDEA, Calle 70 No. 52-21, Medellín, Colombia  
e-mail: [josedavid@udea.edu.co](mailto:josedavid@udea.edu.co)

system frequency to operational values in the so-called Load Frequency Control (LFC) of power systems. However, traditional frequency control strategies have been developed for power systems with almost complete reliance on conventional energy sources, but penetration of Renewable Energy Sources (RES) may require the participation of these new units in the control loops [2].

Wind is the fastest growing and most widely deployed renewable energy source worldwide [3]. Variable Speed Wind Turbine Generators (VSWTG) are the most popular devices for extracting electrical power from wind. VSWTG operation requires action of electronic power converters, which effectively decouple the rotor angular speed of the wind generating unit from the electrical frequency of the grid. Consequently, VSWTG does not contribute directly to the natural inertial response of the system under frequency disturbances and other operational events [4].

However, the increase of wind generators and the unpredictability and variability associated with the wind resource also raise the difficulty level of the frequency regulation tasks in power systems. In future grid operating normative, the participation of wind turbine generators in system frequency regulation might become mandatory. Hence, several studies have been proposed about control strategies for the active inclusion of VSWTG in LFC loops. Complete reviews can be found in [4–6]. Among many techniques, the required primary reserves for frequency regulation contributions from Wind Turbine generators (WT) can be supplied through de-loaded operation (under the point of maximum power extraction) of the WT and the addition of control loops, emulating the response of conventional units (inertia and droop controllers) [4, 7, 8].

This chapter focuses on analyzing the effects of parameter variations in the frequency regulation structure of power systems involving wind generation. Sensitivity functions are established using linearized models and transfer function representations for the system components. Sensitivity analysis has been previously employed in the assessment of the dynamic performance of power systems. Nanda and Kaul [9] explored the optimal tuning of automatic generation controllers in a multi-area power system with conventional steam generation units. The role of inertia was studied through sensitivity tests in the development of a composite load model with conventional machines [10]. For scenarios considering renewable energy sources, the impacts of damping and inertia in the dynamic performance of grid frequency were studied in [11], where authors analyzed different locations to provide emulated inertia. Additionally, the behavior of Doubly-Fed Induction Generator (DFIG) wind units in power systems was studied using eigenvalue sensitivities about inertia variations [12]. However, these works did not consider an explicit function for system sensitivities. In this regard, transfer functions for power systems frequency regulation elements are developed in [13–16] for conventional-only scenarios, and extended in [7] for assessing the effects of load damping including wind farms.

Amidst this context, this chapter studies the effects of varying different system parameters on the overall performance of the traditional LFC system when including contributions of renewable energy systems such as VSWTG. Through both theoretical analysis and performance simulations, the impact of an inaccurate representation of system inertia is established. Results indicate more robustness to parameter

variations for systems that include wind turbine participation. However, the frequency deviation rate increases when the uncertainty in system parameters grows. This behavior would lead to instability scenarios under frequency disturbances for the power system.

## 2 Modeling of the Variable Speed Wind Turbine Generator Control Loops

The relationship between rotor speed and power for a wind turbine (WT) is inherently non-linear. The maximum power point (MPP) is the operational rotor speed value that causes the maximum power extraction from the WT. Given the non-linear dynamic of the system, the MPP needs to be tracked continually in order to guarantee the efficiency of the WT. The MPP tracking (MPPT) process starts with Eq. (1), which represents the mechanical power of the WT:

$$P_m = \frac{1}{2} \rho A C_p (\lambda_w, \beta_w) v_w^3 \quad (1)$$

where  $A$  denotes the turbine sweeping area,  $\rho$  represents the air density,  $\beta_w$  is the pitch-angle,  $\lambda_w$  is Tip Speed Ratio (TSR),  $C_p (\lambda_w, \beta_w)$  is the performance coefficient for the WT, and  $v_w$  represents the per-unitized values of measured wind speed.

By definition, the TSR is a relation between the tangential speed at the tip of a WT blade and the actual wind speed. Therefore, in per-unit system,  $\lambda_{w,p.u.} = \frac{\omega}{v}$ , with  $v$  and  $\omega$  denoting the rotor speed and the wind speed per-unit for a reference speed of 12 m/s. Additionally, Eq. (2) presents the mechanical torque  $T_{m,p.u.}$  of the WT in per-unit system, where  $\omega_m$  represents the per-unitized values of measured rotor speed,  $C_{p,max}$  is the maximum value of  $C_p (\lambda_w, \beta_w)$ , and  $K_w$  is a constant defined in Eq. (3).

$$T_{m,p.u.} = \frac{0.5 \rho A C_p (\lambda_w, \beta_w) v_w^3}{\omega_m P_{base}} = \frac{K_w C_p v^3}{\omega} \quad (2)$$

$$\text{with } K_w = \frac{0.5 \rho A C_{p,max}}{P_{base}} \quad (3)$$

If wind turbines are contributing to frequency regulation, the linearized representation must include changes of the area frequency  $\Delta f$  and wind speed variations  $v$ . In the same way as the LFC, frequency regulation contributions can come from the variation of mechanical or electrical power in response to grid frequency changes.

Frequency contribution from wind turbines is possible due to the so called de-loaded operation [4]. In this mode, the wind turbine operates under the MPP to generate the active power reserve employed to contribute to frequency control tasks. This active power reserve  $P_{cont}$  (p.u.) is:

$$P_{cont} = P_{MPP} - P_{und} = (1 - X_u) K_{wind} \omega^3 \tag{4}$$

where  $\omega$  denotes the rotor speed,  $X_u \in (0, 1)$  is a weighting factor expressing the fraction of maximum power at de-loaded operating point [7],  $P_{und}$  is the de-loaded power,  $P_{MPP}$  is the maximum power extracted at the operating speed, and  $K_{wind}$  is a constant parameter depending on the characteristics of the wind turbine [17]. In operation,  $\omega_{MPP}$  and  $\omega_{und}$  are the rotor angular speeds at  $P_{MPP}$  and  $P_{und}$ , respectively. According to [18], the power  $P_{uref}$  and torque  $\tau_{uref}$  for operating at determined wind speed are:

$$P_{uref} = P_{und} + (P_{MPP} - P_{und}) \frac{(\omega_{und} - \omega)}{(\omega_{und} - \omega_{MPP})} \tag{5}$$

$$= X_u K_{wind} \omega^3 + K_{wind} \omega^3 \frac{(1 - X_u) (\omega_{und} - \omega)}{(\omega_{und} - \omega_{MPP})} \tag{6}$$

$$\tau_{uref} = X_u K_{wind} \omega^2 + K_{wind} \omega^2 \frac{(1 - X_u) (\omega_{und} - \omega)}{(\omega_{und} - \omega_{MPP})} \tag{7}$$

Figure 1 illustrates the model of WT with control loops for frequency contribution from wind turbines. According to this figure, variations in electrical torque  $\Delta\tau_{e,cont}$  can be expressed as:

$$\Delta\tau_{e,cont}(s) = \frac{\Delta P_{e,cont}(s)}{\omega_0} = (-1) \left[ \frac{1/R_w + K_n s}{\omega_0} \right] \Delta f(s) \tag{8}$$

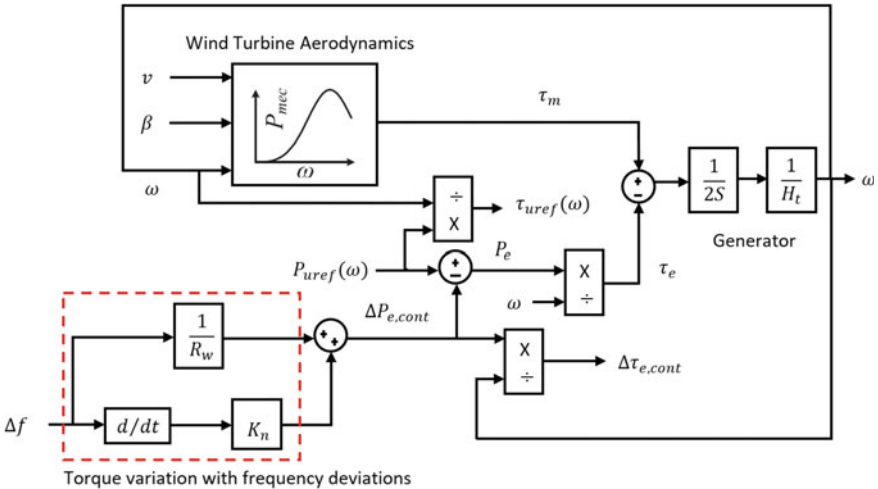


Fig. 1 Model of variable speed WT for LFC support

In Eq. (8),  $\Delta P_{e,cont}$  denotes electrical power variations related to changes in frequency,  $\omega_0$  is the current angular speed of the rotor,  $K_n$  is a parameter weighting the inertia control loop, and  $R_w$  is a parameter similar to the speed droop  $R$  of the LFC regulation. The latter parameters are responsible for inertial emulation from WT, with dynamic performance improving with both low values of  $R_w$  and high values of  $K_n$  [18]. Let the linearized dynamic operating electrical torque be:

$$\Delta\tau_{uref}(s) = \frac{\partial\tau_{uref}}{\partial\omega} \Delta\omega(s) = \left[ 2K_{wind} \omega_0 X_u + 2K_{wind} \omega_0 (1 - X_u) \cdot \frac{(\omega_{und} - \omega_0)}{(\omega_{und} - \omega_{MPP})} - \frac{K_{wind} \omega_0^2 (1 - X_u)}{(\omega_{und} - \omega_{MPP})} \right] \Delta\omega(s). \quad (9)$$

The total variation in electrical torque ( $\Delta\tau_e$ ) can be presented in terms of  $\Delta f(s)$  and  $\Delta\omega(s)$  as follows:

$$\Delta\tau_e(s) = \Delta\tau_{e,cont}(s) + \Delta\tau_{uref}(s) = (-1) \left[ \frac{1/R_w + K_n s}{\omega_0} \right] \Delta f(s) + \frac{\partial\tau_{uref}}{\partial\omega} \Delta\omega(s). \quad (10)$$

Denote  $v_0$  as the wind speed (p.u.) and  $\omega_0$  as the initial angular speed of the rotor at de-loading operating point, and let,  $\lambda_{ref}$  and  $C_{p,ref}$  be the operational values of the tip speed ratio  $\lambda$  and the performance coefficient  $C_p(\lambda, \beta)$  of WT for a reference pitch-angle  $\beta_{ref}$ . The mechanical torque  $\tau_m$  of the turbine is:

$$\tau_m = \frac{K_{wind} C_p v^3}{\omega} \quad (11)$$

From Eq. (11), the linearized mechanical torque  $\Delta\tau_m(s)$  can be expressed as:

$$\begin{aligned} \Delta\tau_m(s) &= \frac{\partial\tau_m}{\partial\omega} \cdot \Delta\omega(s) + \frac{\partial\tau_m}{\partial v} \cdot \Delta v(s) + \frac{\partial\tau_m}{\partial f} \cdot \Delta f(s); \quad \text{with} \quad (12) \\ \frac{\partial\tau_m}{\partial\omega} &= \left( \frac{K_{wind} \zeta v_0^2}{\omega_0} - \frac{K_{wind} C_{p,ref} v_0^3}{\omega_0^2} \right) \\ \frac{\partial\tau_m}{\partial v} &= \left( \frac{3K_{wind} C_{p,ref} v_0^2}{\omega_0} + \frac{K_{wind} \zeta \lambda_{ref} v_0^2}{\omega_0} \right) \\ \frac{\partial\tau_m}{\partial f} &= \left( \frac{\varepsilon K_{wind} K_b v_0^3}{\omega_0} \right). \end{aligned}$$

The expressions for  $\varepsilon = \frac{\partial C_p}{\partial \beta} |_{op}$  and  $\zeta = \frac{\partial C_p}{\partial \lambda} |_{op}$  should be calculated depending on the operational conditions  $\lambda_{ref}$  and  $C_{p,ref}$ . Also,  $K_b = \frac{\Delta\beta}{\Delta f} = \frac{\partial\beta}{\partial f}$ .

For a wind turbine with a inertia  $H_w$ , the swing equation can be employed to obtain an expression for the variations in rotor angular speed  $\Delta\omega$  in terms of the grid frequency variations  $\Delta f$  and wind speed changes  $\Delta v$ . Using the functions for  $\Delta\tau_e(s)$  and  $\Delta\tau_m(s)$ , the power swing equation becomes:

$$\Delta\omega(s) = \frac{\Delta\tau_m(s) - \Delta\tau_e(s)}{2H_w s}. \quad (13)$$

As illustrated in [19], the current parameter values related with active power production in WT can be obtained with small-signal analysis. Denote by  $\Delta P_e$ ,  $\Delta\tau$  and  $\Delta\omega$  the small deviations in electrical power  $P_e$ , electrical torque  $\tau_e$  and the angular rotor speed  $\omega$  respectively. Then,

$$\omega = \omega_0 + \Delta\omega; \quad (14)$$

$$\tau_e = \tau_{e0} + \Delta\tau_e; \quad (15)$$

$$P_e = P_{e0} + \Delta P_e = \tau_e \omega = (\tau_{e0} + \Delta\tau_e)(\omega_0 + \Delta\omega), \quad (16)$$

where  $P_{e0}$ ,  $\tau_{e0}$ , and  $\omega_0$  are the initial values for the corresponding parameters previously mentioned. After expanding Eq. (16) and neglecting the terms of superior order,  $\Delta P_e$  can be expressed in terms of the angular speed and electrical torque deviations as:

$$\Delta P_e = \omega_0 \Delta\tau_e + \tau_{e0} \Delta\omega. \quad (17)$$

In this context, the initial operating electrical torque  $\tau_{e0}$  equates the de-loaded torque  $\tau_{uref}$  presented in Eq. (7). Using the previously developed expressions for  $\Delta\omega$ ,  $\Delta\tau_e$ , and  $\tau_{e0}$ , the linearized electrical power  $\Delta P_e$  for a wind turbine in terms of the grid frequency variations  $\Delta f$  and wind speed changes  $\Delta v$  is:

$$\Delta P_e(s) = \left(\frac{-1}{s+r}\right) \left(\frac{as^2 + bs + c}{qs + 1}\right) \Delta f(s) + \left(\frac{g}{qs + 1}\right) \Delta v(s), \text{ with} \quad (18)$$

$$G_{wf}(s) = \left(\frac{-1}{s+r}\right) \left(\frac{as^2 + bs + c}{qs + 1}\right) \quad (19)$$

$$G_{wv}(s) = \left(\frac{g}{qs + 1}\right). \quad (20)$$

Parameters  $g$ ,  $q$ ,  $r$ ,  $a$ ,  $b$ , and  $c$  are constant terms left omitted because of their extension. They are the result of long algebraic operations among system parameters.

### 3 Extraction of Sensitivity Functions

Frequency regulation can be classified in three main stages according to the nature and timescales of the control efforts: *primary* actions proportional to the frequency deviations, *secondary* actions allowing correction of steady-state errors, and *tertiary* actions related with predefined dispatches and some emergency conditions. These three stages constitute the Load Frequency Control (LFC) system [1, 20]. Grid elements must be modeled for the design of LFC controllers. First order models are

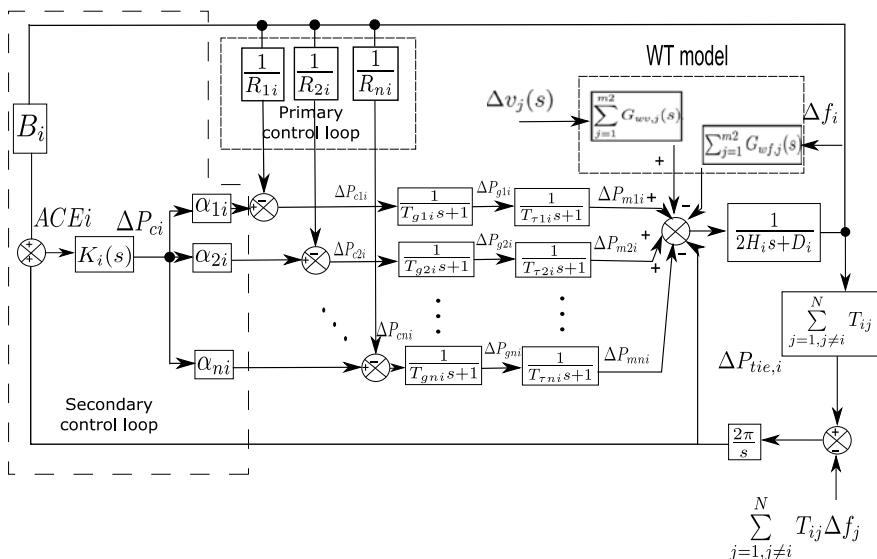


**Fig. 2** Load frequency regulation system with linearized WT model for RES power contributions

assumed for the governor and turbine of conventional units, and for the representation of the frequency response characteristic of any control area in the power system.

Figure 2 illustrates the complete system representation for  $m_1$  conventional units with contribution of  $m_2$  wind generation systems. Note that wind speed variations  $\Delta v_j$  are acting as input parameters, just as the load variations ( $\Delta P_L$ ). From Fig. 2 parameters for the  $i$ -th area are:  $\Delta P_{mki}$  the change in mechanical power of the generator  $k$ ,  $\Delta P_{gki}$  the change in the active power output of generator  $k$ ,  $\Delta P_L$  the load perturbation,  $\Delta f_i$  the frequency change,  $D_i$  the damping coefficient,  $H_i$  the equivalent inertia,  $\Delta P_{cki}$  the control action of the LFC for the  $k$ -th generator,  $T_{ij}$  the power exchange coefficient between area  $i$  and area  $j$ ,  $\Delta P_{tie,i}$  the total change in the power exchanged between area  $i$  and other areas and  $\Delta f_j$  the change in the frequency of area  $j$  connected to area  $i$ . Also,  $B_i$  denotes the bias factor for modulation of the error signal in secondary regulation,  $K_i(s)$  is the transfer function of the secondary controller and  $\alpha_i$  the participation factor of each generator in secondary control. The total inertia  $H_i$  represents the sum of the aggregated inertias of conventional units and wind turbines. Usually, this parameter is calculated empirically, but the analysis of previous works has shown the impacts of inertia in frequency regulation [21, 22]. The sensitivity analysis proposed in this chapter shows the impacts on frequency regulation when the measured value of  $H_i$  is different from the expected. This is also justified as the inertial emulation from wind turbines could lead to inertia variations [13, 14]. From Fig. 2, the total variations on system frequency  $\Delta f$  can be obtained as the linear composition of the individual responses to each input signal. Denote with  $\Delta f_L$  the variations in system frequency with respect to load changes  $\Delta P_L$ . Making  $\Delta v_j = 0$ ,  $\Delta f_L$  is given by:

$$\Delta f_L(s) = \frac{\frac{1}{2H_i s + D} \{-\Delta P_L(s)\}}{1 + \frac{1}{2H_i s + D} \left\{ K(s) + \sum_{i=1}^{m_1} M_i(s) + \sum_{j=1}^{m_2} G_{wf,j}(s) \right\}} \quad (21)$$

In the same way, denoting with  $\Delta f_v$ , the variations in system frequency with respect to wind speed changes  $\Delta v_j$  and making  $\Delta P_L = 0$ , the following expression is obtained:

$$\Delta f_v(s) = \frac{\frac{1}{2H_i s + D} \left\{ \sum_{j=1}^{m_2} G_{wv,j}(s) \Delta v_j(s) \right\}}{1 + \frac{1}{2H_i s + D} \left\{ K(s) + \sum_{i=1}^{m_1} M_i(s) + \sum_{j=1}^{m_2} G_{wf,j}(s) \right\}} \quad (22)$$

Finally, the total variations on system frequency  $\Delta f(s)$  can be expressed from Eqs. (21) and (22), as:

$$\begin{aligned} \Delta f(s) &= \Delta f_L(s) + \Delta f_v(s) \quad (23) \\ &= \frac{\left\{ -\Delta P_L(s) + \sum_{j=1}^{m_2} G_{wv,j}(s) \Delta v_j(s) \right\}}{2H_i s + D + \left\{ K(s) + \sum_{i=1}^{m_1} M_i(s) + \sum_{j=1}^{m_2} G_{wf,j}(s) \right\}} \end{aligned}$$

### 3.1 Sensitivity to Inertia $H_i$

To represent the effects of inertia variations in frequency regulation, the calculation of  $\frac{\partial \Delta f(s)}{\partial H_i}$  is required. Extracting the partial derivative of  $\Delta f$  with respect to  $H_i$  from Eq. (23), the following expression is obtained:

$$\begin{aligned} \frac{\partial \Delta f(s)}{\partial H_i} &= \frac{2s \left[ \Delta P_L(s) - \sum_{j=1}^{m_2} G_{wv,j}(s) \Delta v_j(s) \right]}{\left[ 2H_i s + D + \left\{ K(s) + \sum_{i=1}^{m_1} M_i(s) + \sum_{j=1}^{m_2} G_{wf,j}(s) \right\} \right]^2} \quad (24) \\ &= \{2s\} \left[ \frac{\Delta f(s)}{\left\{ \Delta P_L(s) - \sum_{j=1}^{m_2} G_{wv,j}(s) \Delta v_j(s) \right\}} \right]^2 \left\{ \Delta P_L(s) - \sum_{j=1}^{m_2} G_{wv,j}(s) \Delta v_j(s) \right\} \end{aligned}$$

The unit-less sensitivity function  $S_H$  with respect to total inertia  $H_i$  can be also calculated by definition as:

$$\begin{aligned} S_H &= \frac{d\Delta f(s)}{\Delta f(s)} \bigg/ \frac{dH_i}{H_i} = \frac{\partial \Delta f(s)}{\partial H_i} \cdot \frac{H_i}{\Delta f(s)} \\ &= \frac{\Delta f(s)}{\left\{ \Delta P_L(s) - \sum_{j=1}^{m_2} G_{wv,j}(s) \Delta v_j(s) \right\}} \cdot \{2s H_i\} \quad (25) \end{aligned}$$



In [14], a similar sensitivity analysis was performed for a power system but only with conventional hydraulic machines. From those results, frequency variations  $\Delta f_{base}$  for a purely conventional system (no RES penetration) can be obtained. In this sense, the sensitivity expression  $\Delta f_{base}$  with respect to inertia for conventional power systems is

$$\frac{\partial \Delta f_{base}(s)}{\partial H} = \left[ \frac{\Delta f_{base}(s)}{\Delta P_L(s)} \right]^2 \cdot \Delta P_L(s) \cdot 2s. \quad (26)$$

Similarly, the aforementioned unit-less sensitivity expression  $S_{H,base}$  of  $\Delta f_{base}$  with respect to  $H_{base}$  for a completely conventional power system is [13]:

$$S_{H,base} = \frac{d\Delta f(s)}{\Delta f(s)} \bigg/ \frac{dH_{base}}{H_{base}} = \frac{\partial \Delta f(s)}{\partial H_{base}} \cdot \frac{H_{base}}{\Delta f(s)} = \frac{\Delta f_{base}(s)}{\Delta P_L(s)} 2H_{base}s. \quad (27)$$

The comparison among sensitivities with respect to inertia for power systems with and without wind turbine contributions to frequency variations can be established from Eqs. (24) to (27). As expected, the inclusion of wind turbines means including wind speed in frequency sensitivity through the term  $\sum_{j=1}^{m_2} G_{wv,j}(s) \Delta v_j(s)$  (see Eqs. (24) and (25)). It is expected that the intrinsic unpredictable and variable nature of the wind resource will impact the power generated from renewable units. In consequence, the dynamic characteristics of the frequency regulation are being modified according to the wind profile for a determined inertia value. This will be illustrated through simulation in subsequent sections.

## 4 Stability Analysis of Inertia Sensitivity of LFC with WT

Traditionally, grid frequency variations  $\Delta f(s)$  have been exclusively analyzed under the influence of load disturbances  $\Delta P_L(s)$  [1, 19, 20]. This approximation was developed for systems involving only conventional generation, resulting in the following expression:

$$d\Delta f(s) = \frac{\partial \Delta f(s)}{\partial \Delta P_L(s)} \cdot d\Delta P_L(s). \quad (28)$$

For systems with contribution of wind turbines to frequency regulation, wind speed variations  $\Delta v_j$  need to be considered in the analysis of frequency deviation. Therefore, for a system with frequency regulation contributions from  $m_2$  wind turbines, Eq. (28) becomes:

$$d\Delta f(s) = \frac{\partial \Delta f(s)}{\partial \Delta P_L(s)} \cdot d\Delta P_L(s) + \sum_{j=1}^{m_2} \frac{\partial \Delta f(s)}{\partial \Delta v_j(s)} \cdot d\Delta v_j(s). \quad (29)$$

Nevertheless, the impacts of the system inertia coefficient are not considered neither in Eq. (28) nor Eq. (29). This omission could offer incomplete information, because a loss of generation or an interruption event may result in a variation of the inertia coefficient for a given machine, affecting the aggregated system inertia [23]. These events have a high probability of occurrence in an environment with variable and unpredictable renewable energy sources, where resource intermittence or generation drops may result in changes from the initial inertia calculation [22]. Additionally, inertia could have been estimated from an outdated generation profile. All these phenomena suggest that frequency deviation  $\Delta f$  should consider the effects of the generator inertia coefficient rather than being function of the external disturbances  $\Delta P_L$  and  $\Delta v_j$  exclusively. In consequence, the impact of the inertia coefficient in the grid frequency regulation performance must be determined.

#### 4.1 Extraction of Differential Equation for Frequency Deviation

Assuming mutual independence among  $\Delta P_L$ ,  $\Delta v_j$ , and inertia coefficient  $H_i$ , Eq. 29 is modified by adding variations with respect to  $H_i$ , as follows:

$$d\Delta f(s) = \frac{\partial \Delta f(s)}{\partial \Delta P_L(s)} \cdot d\Delta P_L(s) + \sum_{j=1}^{m_2} \frac{\partial \Delta f(s)}{\partial \Delta v_j(s)} \cdot d\Delta v_j(s) + \frac{\partial \Delta f(s)}{\partial \Delta H_i} d\Delta H_i. \quad (30)$$

From Eq. (24),

$$\frac{\partial \Delta f(s)}{\partial H_i} dH_i = 2s(dH_i) \left[ \frac{\Delta f(s)}{\Delta P_L(s) - \sum_{j=1}^{m_2} G_{wv,j}(s)\Delta v_j(s)} \right]^2 \left\{ \Delta P_L(s) - \sum_{j=1}^{m_2} G_{wv,j}(s)\Delta v_j(s) \right\} \quad (31)$$

Additionally, taking partial derivatives with respect to  $\Delta P_L$  and  $\Delta v_j$  from Eq. 23, we can show that:

$$\frac{\partial \Delta f(s)}{\partial \Delta P_L(s)} = \frac{\Delta f(s)}{\Delta P_L(s)}; \quad \frac{\partial \Delta f(s)}{\partial \Delta v_j(s)} = \frac{\Delta f(s)}{\Delta v_j(s)} \quad (32)$$

Replacing Eqs. (31) and (32) in Eq. (30), we get:

$$d\Delta f(s) = \frac{\Delta f(s)}{\Delta P_L(s)} \cdot d\Delta P_L(s) + \sum_{j=1}^{m_2} \frac{\Delta f(s)}{\Delta v_j(s)} \cdot d\Delta v_j(s) \quad (33)$$

$$+ 2s(dH_i) \left[ \frac{\Delta f(s)}{\Delta P_L(s) - \sum_{j=1}^{m_2} G_{wv,j}(s)\Delta v_j(s)} \right]^2 \left\{ \Delta P_L(s) - \sum_{j=1}^{m_2} G_{wv,j}(s)\Delta v_j(s) \right\}$$

Laplace inverse transformation is employed to get the time domain representation of Eq. (33), resulting in:

$$d\Delta f(t) = L^{-1} \left[ \frac{\Delta f(s)}{\Delta P_L(s)} \cdot d\Delta P_L(s) \right] + L^{-1} \left[ \sum_{j=1}^N \frac{\partial \Delta f(s)}{\partial \Delta v_j(s)} \cdot d\Delta v_j(s) \right] + \dots \quad (34)$$

$$\dots L^{-1} \left\{ \left[ \frac{\Delta f(s)}{\Delta P_L(s) - \sum_{j=1}^{m_2} G_{wv,j}(s) \Delta v_j(s)} \right]^2 \left[ \Delta P_L(s) - \sum_{j=1}^{m_2} G_{wv,j}(s) \Delta v_j(s) \right] \cdot 2sdH_i \right\}.$$

Further, taking integration of Eq. (34), we get  $\Delta f(t)$  as

$$\int d\Delta f(t) = \Delta f(t) = \int L^{-1} \left[ \frac{\Delta f(s)}{\Delta P_L(s)} \cdot d\Delta P_L(s) \right] + \int L^{-1} \left[ \sum_{j=1}^N \frac{\partial \Delta f(s)}{\partial \Delta v_j(s)} \cdot d\Delta v_j(s) \right] + \dots \quad (35)$$

$$\dots L^{-1} \left\{ \left[ \frac{\Delta f(s)}{\Delta P_L(s) - \sum_{j=1}^{m_2} G_{wv,j}(s) \Delta v_j(s)} \right]^2 \left[ \Delta P_L(s) - \sum_{j=1}^{m_2} G_{wv,j}(s) \Delta v_j(s) \right] \cdot 2sdH_i \right\}.$$

Equation (35) presents the total differential equation of frequency deviation  $\Delta f(t)$  in time domain considering inertia effects. In order to determine the impacts of the inertia coefficient, a stability analysis of  $\Delta f(t)$  is presented in the following subsection.

## 4.2 Stability Analysis

After a disturbance, all characteristic poles of the transfer function of a power system are located on the left half-plane in the  $s$ -domain if the system is stable. In this case, the finite time-domain input signals  $\Delta v_j(t)$  and  $\Delta P_L(t)$  would not be producing infinite time-domain responses on system output  $\Delta f(t)$ . From control theory, that is equivalent to show that the norm of the transfer function of the system is bounded. From Eq. (35), this would represent that the transfer functions listed in Eq. (36) are already bounded:

$$\left\{ \begin{array}{l} \left\| \frac{\Delta f(s)}{\Delta P_L(s) - \sum_{j=1}^{m_2} G_{wv,j}(s) \Delta v_j(s)} \right\| \\ \left\| \frac{\Delta f(s)}{\Delta P_L(s)} \right\| \\ \left\| \frac{\sum_{j=1}^N \Delta f(s)}{\Delta v_j(s)} \right\| \end{array} \right\} < \infty \text{ for } \forall t \in (0, \infty) \quad (36)$$

Moreover, frequency regulation in power systems is designed to keep  $\Delta f(t)$  inside a determined finite band despite variations in  $\Delta v_j$  and  $\Delta P_L$ . Assuming an stable

system, the bounds of frequency variations should be determined. Considering both  $\Delta v_j$  and  $\Delta P_L$  as step functions, and using triangle inequality properties in the expression of Eq. (35) we get:

$$\begin{aligned}
\|\Delta f(t)\| &\leq \left\| \int L^{-1} \left[ \frac{\Delta f(s)}{\Delta P_L(s)} \cdot d\Delta P_L(s) \right] + \int L^{-1} \left[ \sum_{j=1}^{m_2} \frac{\Delta f(s)}{\Delta v_j(s)} \cdot d\Delta v_j(s) \right] + \dots \right. \\
&\quad \left. \dots \int L^{-1} \left\{ \left[ \frac{\Delta f(s)}{\Delta P_L(s) - \sum_{j=1}^{m_2} G_{wv,j}(s)\Delta v_j(s)} \right]^2 \cdot \left[ \Delta P_L(s) - \sum_{j=1}^{m_2} G_{wv,j}\Delta v_j(s) \right] \cdot 2sdH_i \right\} \right\| \\
&\leq \left\| \int L^{-1} \left\{ \left\| \frac{\Delta f(s)}{\Delta P_L(s)} \right\| d\Delta P_L(s) \right\} \right\| + \left\| \int L^{-1} \left\{ \left\| \sum_{j=1}^{m_2} \frac{\Delta f(s)}{\Delta v_j(s)} \right\| \left\| \sum_{j=1}^{m_2} d\Delta v_j(s) \right\| \right\} \right\| + \dots \\
&\quad \dots \left\| \int L^{-1} \left\{ \left\| \left[ \frac{\Delta f(s)}{\Delta P_L(s) - \sum_{j=1}^{m_2} G_{wv,j}\Delta v_j(s)} \right]^2 \right\| \left\| \left[ \Delta P_L(s) - \sum_{j=1}^{m_2} G_{wv,j}\Delta v_j(s) \right] \cdot 2sdH_i \right\| \right\} \right\| \\
&\leq \left\| \int L^{-1} [\kappa d\Delta P_L(s)] \right\| + \left\| \int L^{-1} \left[ \eta \sum_{j=1}^{m_2} d\Delta v_j(s) \right] \right\| + \dots \\
&\quad \dots \left\| \int L^{-1} \left\{ \rho^2 \left[ \Delta P_L(s) - \sum_{j=1}^{m_2} G_{wv,j}\Delta v_j(s) \right] \cdot 2sdH_i \right\} \right\| \\
&\leq \left\| \int \kappa \cdot 1(t-t_0)d\Delta P_L \right\| + \left\| \int \eta \cdot 1(t-t_0) \sum_{j=1}^{m_2} d\Delta v_j \right\| + \dots \\
&\quad \dots \left\| \int \rho^2 \cdot \left[ 1(t-t_0)\Delta P_L - \sum_{j=1}^{m_2} \left( \frac{g_j}{q_j} \right) \cdot e^{-\left(\frac{1}{q_j}\right)t} \Delta v_j \right] 2sdH_i \right\| \\
&\leq \kappa \|\Delta P_L\| + \eta \left\| \sum_{j=1}^{m_2} \Delta v_j \right\| + \rho^2 \|H_i\| \left\| \left[ \Delta P_L - \sum_{j=1}^{m_2} \left( \frac{g_j}{q_j} \right) \cdot e^{-\left(\frac{1}{q_j}\right)t} \Delta v_j \right] \right\| \quad (37)
\end{aligned}$$

where  $\kappa = \left\| \frac{\Delta f(s)}{\Delta P_L(s)} \right\|$ ,  $\eta = \left\| \sum_{j=1}^N \frac{\Delta f(s)}{\Delta v_j(s)} \right\|$  and  $\rho = \left\| \left[ \frac{\Delta f(s)}{\Delta P_L(s) - \sum_{j=1}^N G_{wv,j}\Delta v_j(s)} \right] \right\|$  represent the respective bounded magnitudes of the transfer functions established in Eq. (36). Also,  $L^{-1}[1/s] = 1(t-t_0)$ , with  $1(t-t_0) = 1$  when  $t \geq t_0$ . In this way,  $\|1(t-t_0)\| = 1$ . Therefore, the system remains stable when the effects of inertia variations are considered.

In the same way, the output frequency deviation  $\Delta f$  of the traditional power system model without considering inertia effects is given as [23]:

$$\|\Delta f_{base}(t)\| \leq \kappa_{base} \|\Delta P_L\| \quad (38)$$

The expressions in Eqs. (37) and (38) show that the frequency deviations in both cases remain bounded when a stable power system is considered. However, it is

also evident that the boundaries are different. The limits of the conventional model depend on the boundaries of load disturbance  $\Delta P_L$ . However, the consideration of inertia effects and wind turbine integration to frequency regulation affects the boundaries of frequency deviations. In this case, the limits depend on factors such as load disturbance, variations in wind speed, system configuration, and the specific value of  $H_i$ .

## 5 Simulation Results and Discussion

A modified version of the WSCC 9-bus power system [1] was employed for simulating wind turbine contribution in the LFC for a multi-area power system. For the system of Fig. 3, 20% of conventional generation in Area III was replaced by a wind farm. The wind farm was formed by 32 DFIG WT of 2 MW each, whose model parameters were shown in Table 2. The system was modeled as indicated in Fig. 1, and several case studies were analyzed.

### 5.1 Case 1: Frequency Response for a Load Step Change

A step change of 10% is applied to the simulated system at  $t = 0$  s. The system with a reduced inertia was simulated without wind, and with increasing constant wind speed (5 and 10 m/s) as disturbance. Contribution of wind turbines in frequency

**Fig. 3** WSCC 9-bus system multi-area partitioning. The modified system parameters are summarized in Table 1, considering an hydraulic machine and two gas units. The Power Base was set at 100 MVA

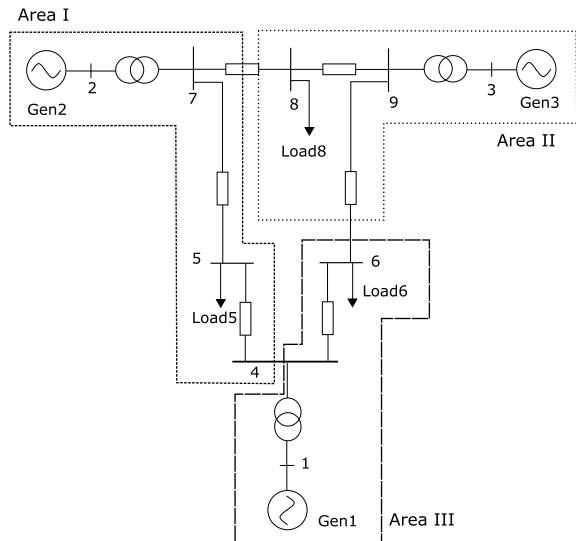


**Table 1** WSCC 9 bus system parameters [1]

Parameter	Value	Parameter	Value	Parameter	Value
$H_1$	23.64 s	$T_{12}$	2.064 p.u.	$R_1$	2 p.u.
$H_2$	6.4 s	$T_{13}$	6.1191 p.u.	$R_2$	10 p.u.
$H_3$	1.505 s	$T_{23}$	14.4353 p.u.	$R_3$	7.5019 p.u.
$MVA_{nom1}$	247.5	$D1, D2, D3$	0.8	$B_1$	2.8 s
$MVA_{nom2}$	192	$Tg1, Tg2, Tg3$	0.2	$B_2$	10.8 s
$MVA_{nom3}$	128	$T\tau1, T\tau2, T\tau3$	0.3	$B_3$	8.3 s

**Table 2** Wind-turbine model simulation parameters [25]

Parameter	Value	Parameter	Value
$P_{nom}$	2 MW	$R_s$	0.00491 p.u.
$V_{nom}$	966 V	$X_{ls}$	0.09273 p.u.
$K_1$	5000 Nm	$X_m$	3.96545 p.u.
$K_2$	2000 Nm	$R_r$	0.00552 p.u.
$T_w$	1	$X_{lr}$	0.1 p.u.
$K_a$	500	$H$	4.5 s
$T_a$	20	$J$	506.61 Kg m <sup>2</sup>

regulation is not being considered. Fig. 4 presents the grid frequency deviations for this case. Frequency nadir is lower for the system with reduced inertia and no wind. Despite the wind being considered exclusively as disturbance, the effects of the wind power injections help to improve the frequency characteristic of the system. Wind power production increases with higher speeds. However, higher speeds may lead to a more oscillatory response, as seen from the curve for a speed of 10 m/s.

## 5.2 Case 2: Frequency Response for a Load Step Change and WT Contribution to LFC

For the previous example, contribution of wind turbines in frequency regulation is now being considered as constant in every case. Figure 5 presents the grid frequency deviations for this case. Again, we can see how the lower frequency nadir is given for the case without active power injections from RES. Response is similar as the one shown in Fig. 4; however, the contribution of wind turbines to frequency regulation provided a smoother response in grid frequency deviation. Again, a higher speed and oscillatory response even with inertia emulation from wind turbines are concerning.

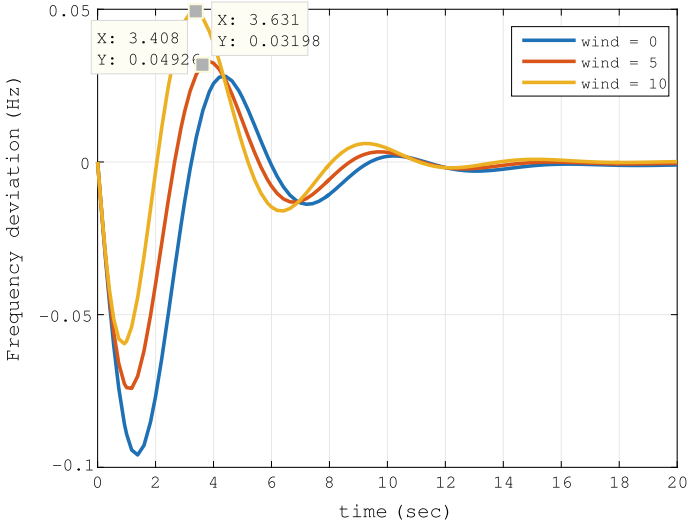


Fig. 4 Case 1: Frequency response without contribution of WT and increasing wind speed

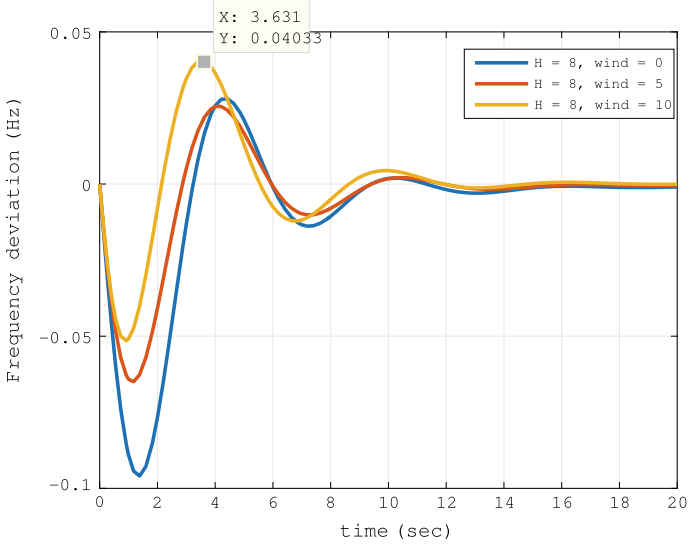
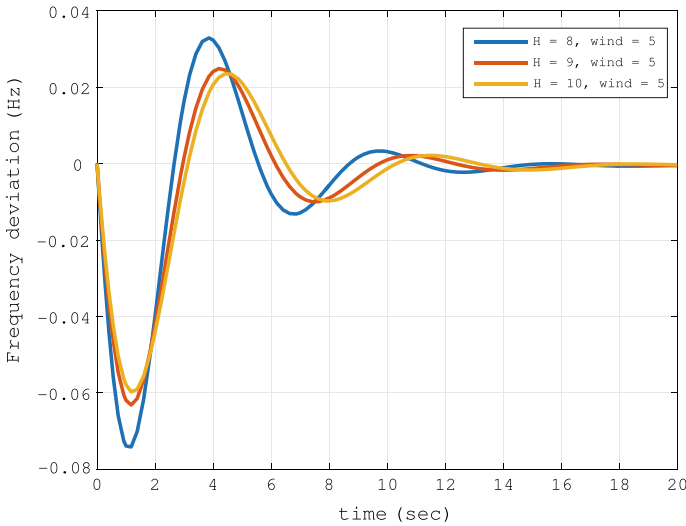


Fig. 5 Case 2: Frequency response with constant contribution of WT and increasing wind speed



**Fig. 6** Case 3: Frequency response with constant wind speed and increasing contribution of WT

### 5.3 Case 3: Frequency Response for a Load Step Change and Increasing Wind Contribution to LFC

A step change of 10% is applied to the simulated system at  $t = 0$  s. Contribution of wind turbines in frequency regulation is being increased (0–10% and 20%) in every case by modifying loop parameters. The system with a reduced inertia was simulated with a constant wind speed of 5 m/s. Figure 6 presents the grid frequency deviations for this case. Here, the effects of the increased inertia with the contribution of wind turbines are evident. However, these effects are being shown with the assumption of constant wind speed.

### 5.4 Case 4: Frequency Response with Constant Wind Speed and Increasing Contribution of WT After Unstable Conditions

For this case, one of the system poles was changed to a value in the right half-plane of the  $s$ -domain. This caused an unstable response in frequency deviations. The same conditions of Sect. 5.3 are applied in this case and the resulting responses are plotted in Fig. 7. The system took longer time in reaching unstable conditions when wind turbines contributed to grid frequency regulation. Wind speed was kept as constant value of 5 m/s. Variability in wind speed may lead to a faster unstable mode.



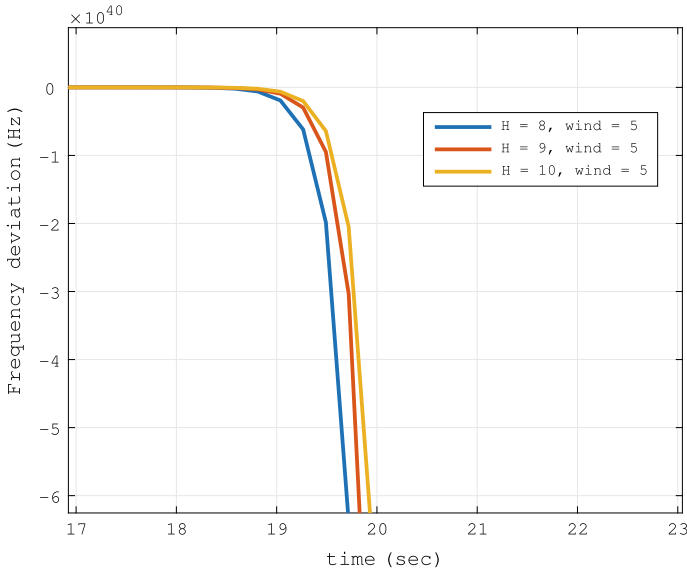


**Fig. 7** Case 4: Frequency response with constant wind speed and increasing contribution of WT, starting from unstable case

### 5.5 Case 5: Frequency Response with a Simulated Wind Profile and Increasing Contribution of WT

The power generation in wind units depends on the wind profile. Wind speed is highly variable and unpredictable, causing fluctuations on wind power generation and frequency deviations. A wind speed profile was simulated with data obtained from the database of Virgin Islands [24]. Load disturbance was not considered, just wind speed. The resultant responses are plotted in Fig. 8, while contribution of wind turbines in frequency regulation is increased (0–10% and 20%). According to Fig. 8, the curves with higher inertia contributions from wind turbines presented smaller peaks than the purely conventional system. In consequence, frequency deviation had a better performance with contribution of RES despite the inherent variability of the wind speed.

### 5.6 Case 6: Frequency Response with a Simulated Wind Profile and Load Disturbance

The same conditions of the immediately previous case were replicated, but now a step load disturbance of 10% was applied at  $t = 50$  s. The contributions of wind turbines make the system more robust to disturbance action, even under the effects

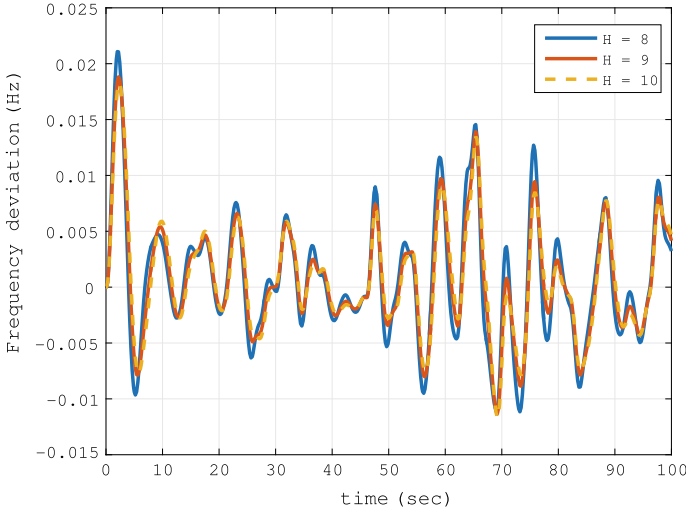


**Fig. 8** Case 5: Frequency response with a simulated wind profile and increasing contribution of WT

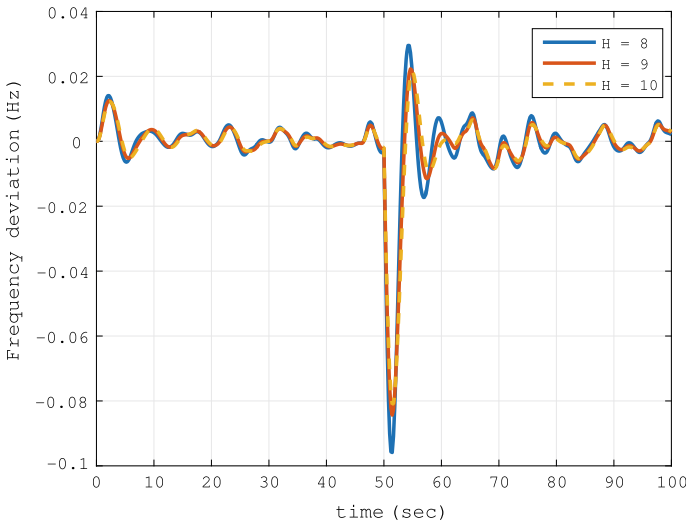


**Fig. 9** Case 6: Frequency response with a simulated wind profile and increasing contribution of WT, and load disturbance  $\Delta P_L = 0.1$  at  $t = 50$  s

of variable wind speed (see Fig. 9). Starting from an stable case, the consideration of inertia variations maintains the stability of the system. This is expected from Eq. (35), and the analysis of Sect. 4.2. The dynamic characteristics of grid frequency deviations can actually improve with a higher value of inertia coefficient.

## 6 Conclusions

This chapter addressed the effects of inertia variations for power systems with integrated wind units. The system transfer functions were obtained from a linearized wind turbine model. The mathematical relationships were formulated to analyze the sensitivity and stability regarding inertia coefficient  $H$ . These expressions were verified through simulation of several cases under different stability conditions and disturbances in wind speed and load.

Simulations have shown a better and smoother response of frequency deviations for the cases with contributions of wind turbines in comparison with the basic case of the purely conventional system. These improvements on frequency response provide a better power quality. Actually, results indicate a better performance of the frequency response for higher contributions of wind turbines to system inertia. Moreover, results suggest more robustness to parameter variations of systems with wind turbine participation. However, the frequency deviation rate increases when the uncertainty of system parameters grows. This behavior would lead to instability scenarios under frequency disturbances for the power system.

With the growing development of intermittent renewable energy sources and its integration of the electrical grid, renewable energy will take more responsibility for frequency regulation tasks in the foreseeable future. Therefore, the impact of changes in generator inertia coefficient  $H$  on the power system frequency regulation must be accounted. We showed, both with theoretic and simulation analyses, that when including the wind generation system into the control loop, an inaccurate generator inertia coefficient  $H$  has a relatively small impact when the power system is inherently stable; while the system frequency deviation may be accelerated when the power system is indeed unstable after disturbance.

In future works, the analysis of the impacts of the combination of the frequency sensitivities with respect to the main system parameters should be explored. This would include parameter such as generator inertia coefficient  $H$ , the governor speed coefficient  $R$  and load-damping coefficient  $D$ . Their effects on the regulation of power system frequency response and stability studies in LFC should be explored together rather than considering them individually.

**Acknowledgements** Colciencias supported contributions of J. Patiño through the program “Convocatoria 528—Convocatoria Nacional para Estudios de Doctorados en Colombia 2011”.

## References

1. Anderson PM, Fouad AA (2002) Power system control and stability. IEEE Press Power Engineering Series. Wiley-IEEE Press
2. DeMarco CL, Baone CA (2014) Chapter 29—Control of power systems with high penetration variable generation. In: Jones LE (ed) Renewable energy integration. Academic Press, Boston, pp 369–379
3. REN21 (ed) (2017) Renewables 2017 global status report. REN21 Secretariat, Paris

4. Vidyanandan KV, Senroy N (2013) Primary frequency regulation by deloaded wind turbines using variable droop. *IEEE Trans Power Syst* 28(2):837–846
5. Díaz-González Francisco, Hau Melanie, Sumper Andreas, Gomis-Bellmunt Oriol (2014) Participation of wind power plants in system frequency control: Review of grid code requirements and control methods. *Renew Sustain Energy Rev* 34:551–564
6. Dreidy M, Mokhlis H, Mekhilef S (2017) Inertia response and frequency control techniques for renewable energy sources: a review. *Renew Sustain Energy Rev* 69:144–155
7. Pradhan C, Bhende CN (2017) Frequency sensitivity analysis of load damping coefficient in wind farm-integrated power system. *IEEE Trans Power Syst* 32(2):1016–1029
8. Ruiz S, Patino J, Espinosa J (2018) PI and LQR controllers for frequency regulation including wind generation. *Int J Electr Comput Eng (IJECE)* 8(6)
9. Nanda J, Kaul BL (1978) Automatic generation control of an interconnected power system. *Proc Inst Electr Eng* 125(5):385–390(5)
10. Pereira L, Kosterev D, Mackin P, Davies D, Undrill J, Zhu W (2002) An interim dynamic induction motor model for stability studies in the WSCC. *IEEE Trans Power Syst* 17(4):1108–1115
11. Borsche TS, Liu T, Hill DJ (2015) Effects of rotational Inertia on power system damping and frequency transients. In: 2015 54th IEEE conference on decision and control (CDC), Dec 2015, pp 5940–5946
12. Gautam D, Vittal V, Harbour T (2009) Impact of increased penetration of DFIG-based wind turbine generators on transient and small signal stability of power systems. *IEEE Trans Power Syst* 24(3):1426–1434
13. Huang Hao, Li Fangxing (2013) Sensitivity analysis of load-damping characteristic in power system frequency regulation. *IEEE Trans Power Syst* 28(2):1324–1335
14. Huang H, Li F (2014) Sensitivity analysis of load-damping, generator inertia and governor speed characteristics in hydraulic power system frequency regulation. In: 2014 Australasian Universities power engineering conference (AUPEC), Sept 2014, pp 1–6
15. Patino J, Valencia F, Espinosa J (2017) Sensitivity analysis for frequency regulation in a two-area power system. *Int J Renew Energy Res* 7(2):700–706
16. Patiño J, López JD, Espinosa J (2018) Analysis of control sensitivity functions for power system frequency regulation. In: Figueroa-García JC, López-Santana ER, Rodríguez-Molano JI (eds) *Applied computer sciences in engineering*, vol 915. Springer International Publishing, Cham, pp 606–617
17. Thomsen SC (2006) Nonlinear control of a wind turbine, ME thesis. PhD thesis, Technical University of Denmark
18. Delille G, Francois B, Malarange G (2012) Dynamic frequency control support by energy storage to reduce the impact of wind and solar generation on isolated power system's inertia. *IEEE Trans Sustain Energy* 3(4):931–939
19. Kundur P (1994) *Power system stability and control*. McGraw-Hill Professional
20. Bevrani H (2014) *Robust power system frequency control*. Power electronics and power systems, 2 edn. Springer
21. Ulbig Andreas, Borsche Theodor S, Andersson Gran (2014) Impact of low rotational inertia on power system stability and operation. *IFAC Proc Vol* 47(3):7290–7297
22. Tielens Pieter, Van Herterem Dirk (2016) The relevance of inertia in power systems. *Renew Sustain Energy Rev* 55:999–1009
23. Huang Hao (2014) *Studies of economics and stability with variable generation and controllable load*. PhD thesis, University of Tennessee

24. Roberts O, Andreas A (1997) United States Virgin Islands: St. Thomas (Bovoni); St. Croix (Longford)
25. Moore IF (2012) Inertial response from wind turbines. PhD thesis, Cardiff University, Cardiff